

Double-Regge-pole analysis of $K^+n \rightarrow K^+\pi^-p$ at 9 GeV/c*

W. L. Yen and F. T. Meiere

Indiana University-Purdue University at Indianapolis, Indianapolis, Indiana 46205

D. D. Carmony, D. Cords,† A. F. Garfinkel,
F. J. Loeffler, R. L. McIlwain, and L. K. Rangan
Purdue University, Lafayette, Indiana 47907

R. L. Lander, D. E. Pellett, and P. M. Yager
University of California at Davis, Davis, California 95616
(Received 24 May 1973)

We report on a study of the diffraction dissociation of the neutron from the reaction $K^+n \rightarrow K^+\pi^-p$ at 9 GeV/c. The data are compared with a double-Regge-pole-exchange model of Berger. Good agreement with our data is obtained for distributions in $M(p\pi^-)$, $M(K^+\pi^-)$, $t_{n,p}$, the Toller angle, the Treiman-Yang angle, the proton production angle, and the Van Hove angle. The $p\pi$ mass dependence of t_{KK} is also well described.

I. INTRODUCTION

In this paper we present data on the reaction

$$K^+n \rightarrow K^+\pi^-p \quad (1)$$

at 9 GeV/c and use a double-Regge-pole-exchange model (DRPEM) to describe the data. The advantage of the DRPEM is that it has the same simple form as a single-Regge-pole-exchange model and the parameters it uses can be taken from those determined by two-body or quasi-two-body reactions. In addition, the double-Regge approach provides an understanding of the entire reaction resulting in a three-body final state; it yields distributions in all relevant kinematical variables, not merely fits to the Dalitz plot or to one Chew-Low plot.

The double-Regge approach is an extension of a single-Regge-pole-exchange model made by several groups in recent years.¹⁻⁴ Phenomenological fits of double-Regge-pole models to processes with three-particle final states have been achieved by many groups.^{2,4-9} We shall adopt the model used by Berger in Ref. 6. Of particular interest is the interpretation of the low-mass π^-p enhancement as a result of peripheral dynamics or as a resonant state, or perhaps both. In the same reaction at 12 GeV/c, Lissauer *et al.*¹⁰ interpret this enhancement in terms of $P_{1/2}$, $D_{3/2}$, and $F_{5/2}$ resonance contributions.

II. EXPERIMENTAL RESULTS

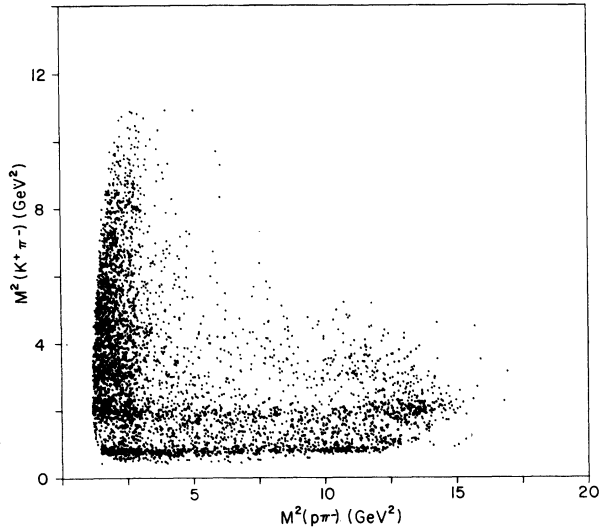
The data were obtained through a 400 000-picture exposure of the Brookhaven National Laboratory 80-in. deuterium-filled bubble chamber to a 9-GeV/c rf-separated K^+ beam. The pathlength

equivalent of the exposure is 10 events/ μb . Of 85 000 three- and four-prong events measured on SMP's (scanning and measuring projectors) and processed by the TVGP-SQUAW analysis programs, 4838 fitted to the four-constraint $K^+\pi^-p$ final-state hypothesis, with a χ^2 probability of greater than 0.1%. In the case of four-prong events, we demand that the spectator proton have a momentum less than 0.3 GeV/c. The contamination to this final state is believed to be negligible. The cross section for this final state is $505 \pm 20 \mu\text{b}$.

Figure 1 shows the Dalitz plot for the reaction $K^+n \rightarrow K^+\pi^-p$. The plot shows that this reaction is separated into two main parts: (a) K^* production [especially $K^*(890)$ and $K^*(1420)$] and (b) diffraction dissociation of the neutron, the K meson remaining unexcited. The K^* production has been presented earlier.¹¹⁻¹³

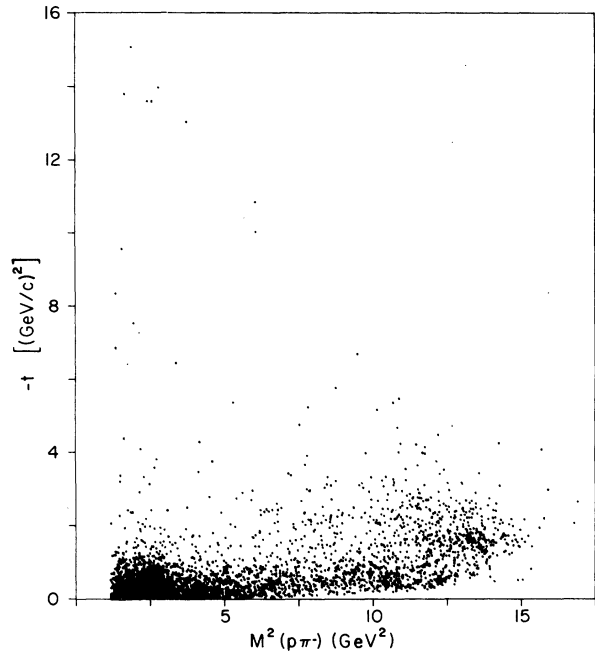
Figure 2 shows the $p\pi^-$ mass spectrum; its major feature is a large, broad mass enhancement centered near $M(p\pi^-) \approx 1.4$ GeV which drops off sharply at $M(p\pi^-) \approx 1.7$ GeV. This large enhancement has been also observed in several other experiments.^{8-10,14} This effect seems to be a direct effect in $M(p\pi^-)$ rather than a reflection of an effect in $M(K\pi^-)$, since the $M(p\pi^-)$ enhancement extends well beyond the K^* bands. The cross section for this enhancement above background is $270 \pm 20 \mu\text{b}$. The cross section of the same enhancement from the same reaction at 12 GeV/c is $240 \pm 13 \mu\text{b}$.¹⁵

Figure 3 shows the Chew-Low plot which relates t , the momentum transfer squared between the incoming and outgoing K^+ mesons, with $M^2(p\pi^-)$. The low- $M(p\pi^-)$ enhancement is produced peripherally although it does extend to fairly high t

FIG. 1. Dalitz plot for the reaction $K^+n \rightarrow K^+\pi^-p$.

$[\approx 1 \text{ (GeV/c)}^2]$.

Figure 4 shows the differential cross section $d\sigma/dt'$ for $M(p\pi^-)$ below 1.8 GeV, where $t' = t_0 - t$ and t_0 is the kinematic lower limit of t . The distribution evidently cannot be fitted by a single exponential linear in t' , but can be adequately fitted by the sum of two exponentials,

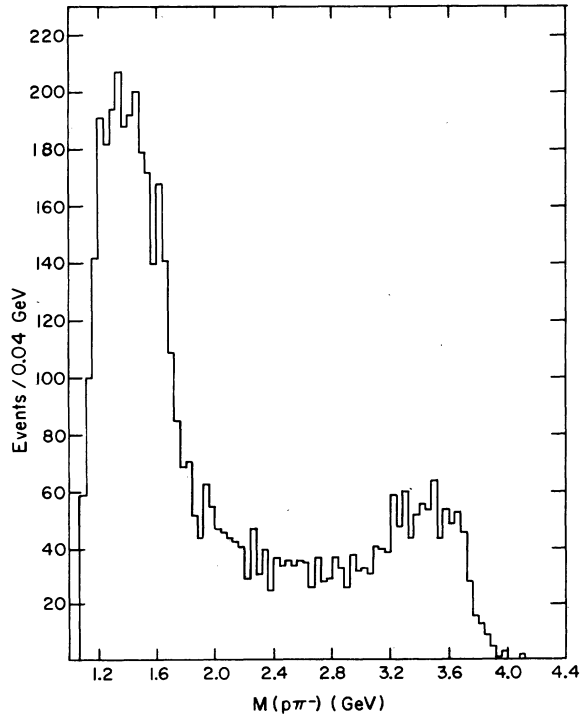
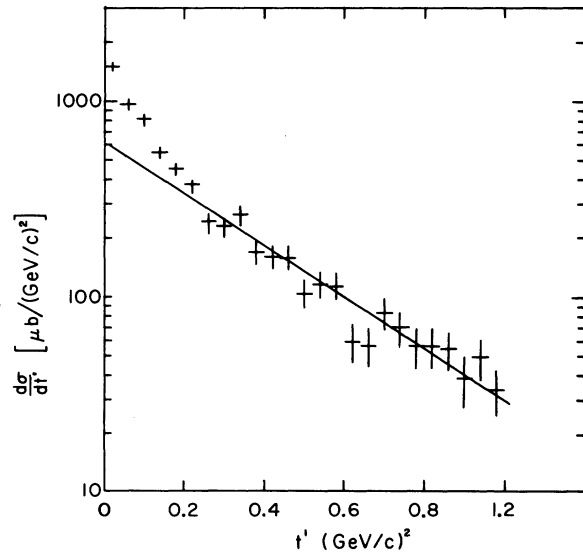
FIG. 3. Chew-Low plot $M^2(p\pi^-)$ vs $-t$ for $K^+n \rightarrow K^+\pi^-p$.

$$\frac{d\sigma}{dt'} = A_1 e^{-b_1 t'} + A_2 e^{-b_2 t'}, \quad (2)$$

with

$$A_1 = 1200 \pm 120 \mu\text{b}/(\text{GeV}/c)^2,$$

$$A_2 = 616 \pm 50 \mu\text{b}/(\text{GeV}/c)^2,$$

FIG. 2. $M(p\pi^-)$ distribution for all $K^+n \rightarrow K^+\pi^-p$ events.FIG. 4. $d\sigma/dt'$ vs t' for $K^+n \rightarrow K^+\pi^-p$ events such that $M(p\pi^-) < 1.8 \text{ GeV}$. The straight line corresponds to an exponential with slope equal to 3 $(\text{GeV}/c)^{-2}$.

$$b_1 = 14 \pm 2 \text{ (GeV/c)}^{-2},$$

$$b_2 = 3.0 \pm 0.2 \text{ (GeV/c)}^{-2}.$$

Figure 5 shows the differential cross sections $d\sigma/dt'$ in the following 0.2-GeV bins of $M(p\pi^-)$: (a) $1.1 < M(p\pi^-) < 1.3$ GeV, (b) $1.3 < M(p\pi^-) < 1.5$ GeV, (c) $1.5 < M(p\pi^-) < 1.7$ GeV. The fit to a single linear exponential

$$\frac{d\sigma}{dt'} = A e^{-bt'} \quad (3)$$

for $t' < 0.2 \text{ (GeV/c)}^2$ gives $b = 12 \pm 1$, 7 ± 1 , and $4 \pm 1 \text{ (GeV/c)}^{-2}$ in the three $M(p\pi^-)$ bins (a), (b), and (c), respectively. The dependence of the $d\sigma/dt'$ distributions on $M(p\pi^-)$ has also been seen in many other experiments.^{6,8,10} In particular in the same reaction at 12 GeV/c, Lissauer *et al.*¹⁰ find slopes of 14, 8, and 3.5 with comparable errors.

In this paper we shall interpret the above features with the double-Regge model used by Berger.⁶

III. DOUBLE-REGGE MODEL

The diagram corresponding to the amplitude used to parametrize the data in this experiment is shown in Fig. 6(a). The double-Regge amplitude squared may be written in the following form⁶:

$$|A|^2 = N_0 |R_\pi(t_{np})|^2 \left(\frac{\bar{s}_{p\pi}}{s_{0p\pi}} \right)^{2\alpha_\pi} |R_p(t_{KK})|^2 \left(\frac{\bar{s}_{K\pi}}{s_{0p}} \right)^2, \quad (4)$$

where

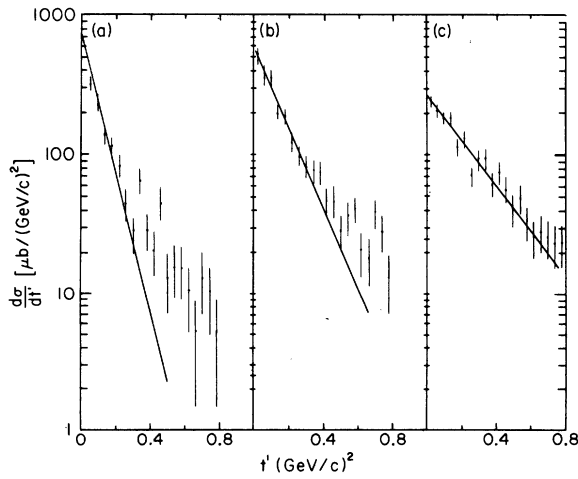


FIG. 5. $d\sigma/dt'$ vs t' for three ranges of $M(p\pi^-)$: (a) $1.1 < M(p\pi^-) < 1.3$ GeV, (b) $1.3 < M(p\pi^-) < 1.5$ GeV, (c) $1.5 < M(p\pi^-) < 1.7$ GeV. The straight lines correspond to exponentials with slopes equal to 12, 7, and 4 $(\text{GeV/c})^{-2}$ for parts (a), (b), and (c) respectively.

$$|R_\pi(t_{np})|^2 = \frac{|t_{np}|}{1 - \cos(\pi\alpha_\pi)} \exp(\lambda t_{np}),$$

$$|R_p(t_{KK})|^2 = \exp(\gamma t_{KK}),$$

$$\bar{s}_{p\pi} = s_{p\pi} - t_{KK} - m_\pi^2 - \frac{1}{2}(m_\pi^2 - t_{np} - t_{KK}),$$

$$\bar{s}_{K\pi} = s_{K\pi} - t_{np} - m_K^2 - \frac{1}{2}(m_\pi^2 - t_{KK} - t_{np}), \quad (5)$$

and

$$\alpha_\pi = \alpha'_\pi(t_{np} - m_\pi^2).$$

N_0 is a normalization constant, m_K and m_π are the masses of kaon and pion, respectively, and λ , γ , $s_{0p\pi}$, s_{0p} , and α'_π are parameters to be determined. The invariants t_{np} , t_{KK} , $s_{p\pi}$, and $s_{K\pi}$ are explained in Fig. 6(a).

All our calculations have been carried out using the Monte Carlo phase-space program FOWL¹⁶ with the function $|A|^2$ as WEIGHT. The values we

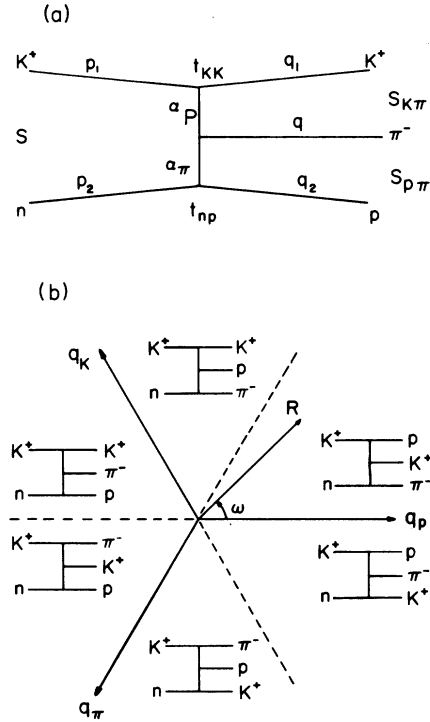


FIG. 6. (a) Double-Regge-pole-exchange diagram we used for the process $K^+n \rightarrow K^+\pi^-p$; α_P denotes the Pomeron and α_π the pion trajectory. The p_i and q_i are four-momenta. $s = (p_1 + p_2)^2$, $s_{K\pi} = (q_1 + q)^2$, $s_{p\pi} = (q + q_2)^2$, $t_{KK} = (q_1 - p_1)^2$, $t_{np} = (q_2 - p_2)^2$. (b) Van Hove longitudinal phase-space plot for $K^+\pi^-p$. q_K , q_π , and q_p are longitudinal momenta of K^+ , π^- , and p in the total center-of-mass system, respectively. An event is represented by a vector \vec{R} in this plot. The vector \vec{R} defines the Van Hove angle ω . Each of the six half-sides is assigned to a different multiperipheral diagram according to the relative values of the c.m. longitudinal momenta.

used for these parameters are¹⁷

$$\lambda = 3.5 \text{ (GeV/c)}^{-2},$$

$$\gamma = 4 \text{ (GeV/c)}^{-2},$$

$$s_{0\pi} = 0.7 \text{ GeV}^2,$$

$$s_{0p} = 1 \text{ GeV}^2,$$

and

$$\alpha'_\pi = 1.2 \text{ GeV}^{-2}.$$

The experimental data and the model have been subjected to the same cuts and selections. These consist in the three cuts $|t_{np}| < 0.8 \text{ (GeV/c)}^2$, $s_{K\pi} > 2.56 \text{ GeV}^2$, and $120^\circ < \omega < 180^\circ$, where ω is the Van Hove angle and is defined in Fig. 6(b). The cut in the Van Hove angle is to comply with the selection of the diagram shown in Fig. 6(a). After the above cuts, we have 1630 events left for analysis. As seen by comparing Figs. 2 and 7(a), however, about 60% of the amount of low-

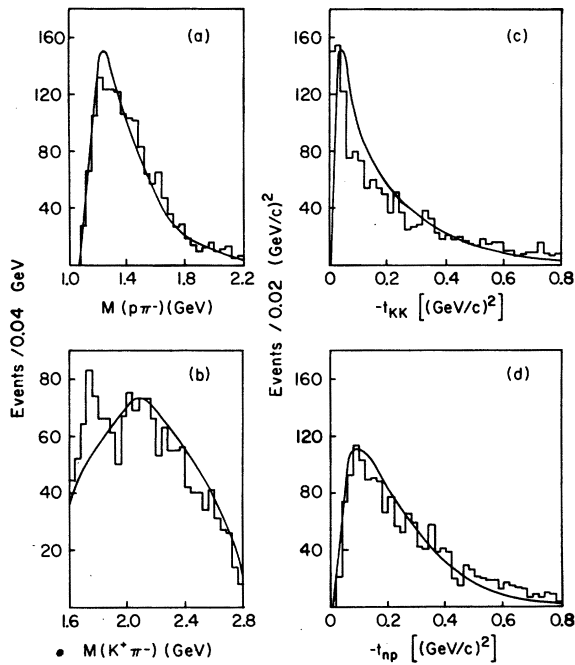


FIG. 7. (a) $M(p\pi^-)$ distribution containing events for which $M(K^+\pi^-) > 1.6 \text{ GeV}$, $|t_{np}| < 0.8 \text{ (GeV/c)}^2$, and $120^\circ < \omega < 180^\circ$. (b) $M(K^+\pi^-)$ distribution containing events for which $|t_{np}| < 0.8 \text{ (GeV/c)}^2$ and $120^\circ < \omega < 180^\circ$. (c) Distribution in the invariant four-momentum transfer squared to the K^+ from the incident K^+ . The plot contains events for which $M(K^+\pi^-) > 1.6 \text{ GeV}$, $|t_{np}| < 0.8 \text{ (GeV/c)}^2$, and $120^\circ < \omega < 180^\circ$. (d) Distribution in the invariant four-momentum transfer squared to the proton from the neutron. The plot contains events for which $M(K^+\pi^-) > 1.6 \text{ GeV}$ and $120^\circ < \omega < 180^\circ$. All curves are from the DRPEM fits.

mass enhancement above background remains after these cuts.

In Figs. 7 and 8 the predictions of the DRPEM are compared with the following commonly studied experimental distributions (not all of which are independent): $M(p\pi^-)$, $M(K^+\pi^-)$, t_{KK} , t_{np} , the Toller angle, the Treiman-Yang angle, the proton production angle, and the Van Hove angle. The Toller angle τ , the Treiman-Yang angle ϕ , and the proton production angle θ are defined by

$$\cos \tau = \frac{(\vec{p}_1 \times \vec{q}_1) \cdot (\vec{p}_2 \times \vec{q}_2)}{|\vec{p}_1 \times \vec{q}_1| |\vec{p}_2 \times \vec{q}_2|} \quad \text{in the } \pi^- \text{ rest frame,}$$

$$\cos \phi = \frac{(\vec{p}_1 \times \vec{q}_1) \cdot (\vec{p}_2 \times \vec{q}_2)}{|\vec{p}_1 \times \vec{q}_1| |\vec{p}_2 \times \vec{q}_2|} \quad \text{in the } K^+\pi^- \text{ rest frame,} \quad (6)$$

$$\cos \theta = \frac{\vec{q}_2 \cdot \vec{p}_2}{|\vec{q}_2| |\vec{p}_2|} \quad \text{in the } p\pi^- \text{ rest frame,}$$

where \vec{p}_i and \vec{q}_i are the four-momenta defined

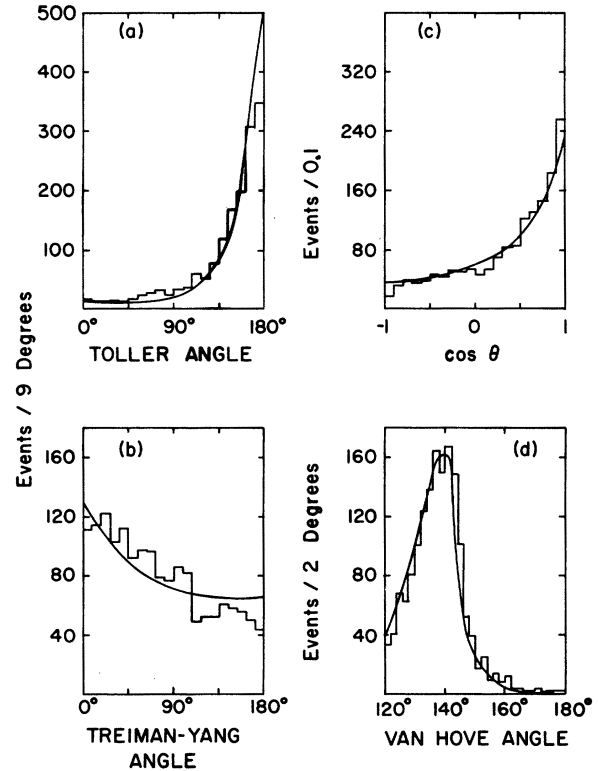


FIG. 8. (a) Distribution in the Toller angle measured in the π^- rest frame. (b) Distribution in the Treiman-Yang angle measured in the $K^+\pi^-$ rest frame. (c) Distribution in the cosine of the proton production angle measured in the $p\pi^-$ rest frame. (d) Distribution in the Van Hove angle measured in the total center-of-mass system. Each of the diagrams contains events for which $M(K^+\pi^-) > 1.6 \text{ GeV}$, $|t_{np}| < 0.8 \text{ (GeV/c)}^2$, and $120^\circ < \omega < 180^\circ$. All curves are from the DRPEM fits.

TABLE I. Mass dependence of the slope of differential cross section.

$M(p\pi^-)$ (GeV)		b (GeV/c) ⁻²	
from	to	Experiment	DRPEM prediction
1.0	1.2	10 ± 1	8.8
1.2	1.3	8 ± 1	7.6
1.3	1.4	7 ± 1	6.2
1.4	1.5	4 ± 1	3.8
1.5	1.6	2 ± 1	3.5

in Fig. 6(a).

The model correctly reproduces the skewed Treiman-Yang angular distribution [Fig. 8(b)] and all other distributions with the exception of the $K\pi$ mass distribution [Fig. 7(b)] in which a residual $K_N(1760)$ signal¹² can be seen and the $-t_{KK}$ distribution [Fig. 7(c)] in the forward direction.¹⁸

We have also studied the slopes of the differential cross sections when plotted against t' . Figure 9 shows t' distributions for various regions of the invariant mass $M(p\pi)$. The straight lines are fits to the data by the expression $d\sigma/dt' = Ae^{-bt'}$ in the region $t' < 0.4$ (GeV/c)². Table I gives the value of b for various $M(p\pi)$ together with the DRPEM predictions. The agreement is quite good.

IV. SUMMARY

The cross section for the reaction $K^+n \rightarrow pK^+\pi^-$ at 9 GeV/c is $505 \pm 20 \mu b$. The reaction can be separated into K^* production and diffraction dissociation of the neutron. The data from the latter part of the reaction are well described by DRPEM. The mass dependence of the slopes of the differential cross section can also be described by the DRPEM.

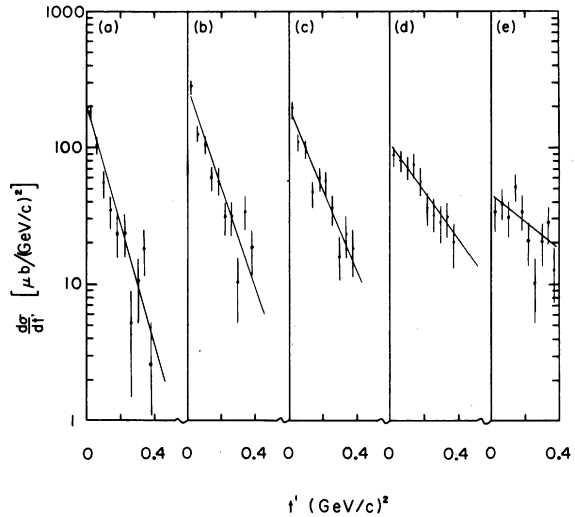


FIG. 9. $d\sigma/dt'$ vs t' for five ranges of $M(p\pi^-)$: (a) $M(p\pi^-) < 1.2$ GeV, (b) $1.2 < M(p\pi^-) < 1.3$ GeV, (c) $1.3 < M(p\pi^-) < 1.4$ GeV, (d) $1.4 < M(p\pi^-) < 1.5$ GeV, (e) $1.5 < M(p\pi^-) < 1.6$ GeV. In addition to the restrictions in $M(p\pi^-)$, events in the diagram are also subjected to the following cuts: $M(K^+\pi^-) > 1.6$ GeV, $|t_{np}| < 0.8$ (GeV/c)², and $120^\circ < \omega < 180^\circ$. The straight lines correspond to exponentials with slopes equal to 10, 8, 7, 4, and 2 (GeV/c)⁻² for parts (a), (b), (c), (d), and (e), respectively.

ACKNOWLEDGMENTS

We wish to thank the physicists and technicians at Brookhaven National Laboratory for their assistance during the exposure, and our engineers, technicians, programmers, and scanners for their tireless efforts. Also, we wish to thank Professor K. Vasavada of IUPUI for helpful discussions.

One of us (W.L.Y.) wishes to thank Indiana University Research Foundation for a fellowship during the summer of 1972.

*Work supported in part by the U. S. Atomic Energy Commission.

†Present address: Deutsches Elektronen-Synchrotron, Notkestieg 1, 2000 Hamburg-52, Germany.

¹N. F. Bali, G. F. Chew, and A. Pignotti, Phys. Rev. Lett. **19**, 614 (1967); Phys. Rev. **163**, 1572 (1967). An extensive list of references to earlier work may be found in G. F. Chew and A. Pignotti, *ibid.* **176**, 2112 (1968).

²Chan Hong-Mo, K. Kajantie, and G. Ranft, Nuovo Cimento **49**, 157 (1967); Chan Hong-Mo *et al.*, *ibid.* **51**, 696 (1967).

³F. Zachariasen and G. Zweig, Phys. Rev. **160**, 1322 (1967); **160**, 1326 (1967).

⁴R. G. Roberts and G. M. Fraser, Phys. Rev. **159**, 1297 (1967).

⁵E. L. Berger, Phys. Rev. **166**, 1525 (1968); Phys. Rev. Lett. **21**, 701 (1968); E. L. Berger, E. Gellert, G. A. Smith, E. Colton, and P. E. Schlein, *ibid.* **20**, 964 (1968); M. L. Ioffredo, G. W. Brandenburg, A. E. Brenner, B. Eisenstein, L. Eisenstein, W. H. Johnson, Jr., J. K. Kim, M. E. Law, B. M. Salzberg, J. H. Scharenguivel, L. K. Sisterson, and J. J. Szymanski, *ibid.* **21**, 1212 (1968).

⁶E. L. Berger, Phys. Rev. **179**, 1567 (1969), and private communication.

⁷J. A. Galdos, C. R. Ezell, J. W. Lamsa, and R. B. Willmann, Phys. Rev. D **2**, 1226 (1970); Nucl. Phys.

- B23, 84 (1971); B26, 109 (1971); C. Fu, Phys. Rev. D 3, 92 (1971).
- ⁸P. Antich, A. Callahan, R. Carson, C. Y. Chien, B. Cox, D. Denegri, L. Ettlinger, D. Feilock, G. Goodman, J. Haynes, R. Mercer, A. Pevsner, L. Resvanis, R. Sekulin, V. Sreedhar, and R. Zdanis, Nucl. Phys. B29, 305 (1971).
- ⁹Y. Cho, M. Derrick, D. Johnson, B. Musgrave, T. Wangler, J. Wong, R. Ammar, R. Davis, W. Kropac, H. Yarger, and B. Werner, Phys. Rev. D 3, 1561 (1971).
- ¹⁰D. Lissauer, A. Firestone, J. Ginestet, G. Goldhaber, and G. H. Trilling, Phys. Rev. D 6, 1852 (1972).
- ¹¹D. Cords, D. D. Carmony, H. W. Clopp, A. F. Garfinkel, R. F. Holland, F. J. Loeffler, H. B. Mathis, L. K. Rangan, J. Erwin, R. L. Lander, D. E. Pellett, P. M. Yager, F. T. Meiere, and W. L. Yen, Phys. Rev. D 4, 1974 (1971).
- ¹²D. D. Carmony, D. Cords, H. W. Clopp, A. F. Garfinkel, R. F. Holland, F. J. Loeffler, H. B. Mathis, L. K. Rangan, J. Erwin, R. L. Lander, D. E. Pellett, P. M. Yager, F. T. Meiere, and W. L. Yen, Phys. Rev. Lett. 27, 1160 (1971).
- ¹³H. W. Clopp, Ph.D. thesis, Purdue University (unpublished).
- ¹⁴R. B. Bell, D. J. Crennell, P. V. C. Hough, W. Karshon, K. W. Lai, J. M. Scarr, T. G. Schumann, I. O. Skillicorn, R. C. Strand, A. H. Bachman, P. Baumel, R. M. Lea, and A. Montwill, Phys. Rev. Lett. 20, 164 (1968); W. E. Ellis, D. J. Miller, T. W. Morris, R. S. Panvini, and A. M. Thorndike, *ibid.* 21, 697 (1968); A. Shapira, O. Benary, Y. Eisenberg, E. E. Ronat, D. Yaffe, and G. Yekutieli, *ibid.* 21, 1835 (1968); R. S. Panvini, T. W. Morris, F. Bomse, W. Burdett, E. Moses, E. Salant, J. Waters, and M. Webster, Bull. Am. Phys. Soc. 15, 659 (1970); D. J. Crennell, K. W. Lai, J. Louie, J. M. Scarr, and W. H. Sims, Phys. Rev. Lett. 25, 187 (1970); Aachen-Berlin-Bonn-CERN-Cracow Collaboration, K. Boesebeck *et al.*, Nucl. Phys. B28, 381 (1971); M. J. Longo, L. W. Jones, D. D. O'Brien, J. C. VanderVelde, M. B. Davis, B. G. Gibbard, M. N. Kreisler, Phys. Lett. 36B, 560 (1971); Aachen-Berlin-Bonn-CERN Collaboration, K. Boesebeck *et al.*, Nucl. Phys. B40, 39 (1972); G. Yekutieli, D. Yaffe, A. Shapira, E. E. Ronat, U. Karshon, and Y. Eisenberg, *ibid.* B40, 77 (1972); Y. T. Oh, S. Y. Fung, A. Kernan, R. T. Poe, T. L. Schalk, and B. C. Shen, Phys. Lett. 42B, 497 (1972).
- ¹⁵A simple phase-space background form was used to estimate the cross sections. The 12-GeV/c data were taken from Lissauer *et al.*, Ref. 10.
- ¹⁶F. James, CERN Report No. 68/15, 1968 (unpublished).
- ¹⁷The parameters $s_{0\pi}$, s_{0p} , and α'_π were taken from Ref. 6. The γ and the additional parameter λ were adjusted to give the best fit to the various distributions. A change of ± 1 in λ and γ does not change the over-all fit considerably.
- ¹⁸The agreement of the $-t_{KK}$ distribution with the prediction is not improved if we remove the $K_N(1760)$ region.

The reaction $pp \rightarrow pp\pi^+\pi^-$ at 205 GeV/c*

M. Derrick, B. Musgrave, P. Schreiner, and H. Yuta

Argonne National Laboratory, Argonne, Illinois 60439

(Received 23 October 1973)

The reaction $pp \rightarrow pp\pi^+\pi^-$ is studied at 205 GeV/c using the 30-in. bubble chamber at the National Accelerator Laboratory. The event selection is discussed in detail and the cross section is measured to be 0.68 ± 0.14 mb. This cross section is higher than one would expect based on a simple power-law extrapolation of lower-energy data. Peripheral production of a low-mass $p\pi^+\pi^-$ system dominates the reaction. The data are consistent with conservation of t -channel helicity.

I. INTRODUCTION

The reaction

$$pp \rightarrow pp\pi^+\pi^- \quad (1)$$

has been extensively studied for momenta from threshold up to 28 GeV/c.¹⁻⁴ The data exhibit a pronounced, low-mass enhancement in the $p\pi^+\pi^-$ system with some suggestion of structure corresponding to isospin- $\frac{1}{2}$ N^* resonance production.^{4,5} Although it is generally asserted on the basis of the existence of the low-mass enhance-

ment and its peripheral nature that the reaction exhibits strong diffractive production of the $p\pi\pi$ system, the total cross section for (1) decreases markedly with increasing beam momentum from 10 to 28 GeV/c, whereas diffractive processes should be nearly independent of beam momentum. We present a study of this reaction at 205 GeV/c and find that the cross section decreases more slowly between 28 and 205 GeV/c than is found for incident momenta below 28 GeV/c, which suggests that diffractive processes are becoming dominant in the several-hundred-GeV energy region.